HHS Public Access

Author manuscript

Biotechnol Bioeng. Author manuscript; available in PMC 2020 July 01.

Published in final edited form as:

Biotechnol Bioeng. 2019 July ; 116(7): 1644–1655. doi:10.1002/bit.26973.

Quantitative Characterization of the Regulation of Iron Metabolism in Glioblastoma Stem-Like Cells using Magnetophoresis

Kyoung-Joo Jenny Park[a,1,3], **James Kim**[a,1], **Thomas Testoff**[a], **Joseph Adams**[a], **Miranda Poklar**[a], **Maciej Zborowski**[b], **Monica Venere**[c,2,4], **Jeffrey J. Chalmers**[a,2,4]

[a]William G. Lowrie Department of Chemical and Biomolecular Engineering, The Ohio State University, 470 CBEC 151 West Woodruff Avenue, Columbus, OH 43210;

[b]Department of Biomedical Engineering, Cleveland Clinic, 9500 Euclid Avenue, Cleveland, OH 44195;

[c]Department of Radiation Oncology and the Comprehensive Cancer Center, The Ohio State University, 514 B Tzagournis Medical Research Facility 420 West 12th Avenue, Columbus, OH 43210

Abstract

This study focuses on different iron regulation mechanisms of glioblastoma (GBM) cancer stem-like cells (CSCs) and non-stem tumor cells (NSTCs) using multiple approaches: cell viability, density and magnetophoresis. GBM CSCs and NSTCs were exposed to elevated iron concentration, and their magnetic susceptibility was measured using Single Cell Magnetophoresis (SCM), which tracks the magnetic and settling velocities of thousands of individual cells passing through the magnetic field with a constant energy gradient. Our results consistently demonstrate that GBM NSTCs have higher magnetic susceptibility distribution at increased iron concentration compared to CSCs, and we speculate that it is because CSCs have the ability to store a high amount of iron in ferritin, whereas the free iron ions inside the NSTCs lead to higher magnetic susceptibility and reduced cell viability and growth. Further, their difference in magnetic susceptibility has led us to pursue a separation experiment using a Quadrupole magnetic separator (QMS), a novel microfluidic device that uses a concentric channel and permanent magnets in special configuration to separate samples based on their magnetic susceptibilities. GBM CSCs and NSTCs were exposed to elevated iron concentration, stained with two different trackers, mixed and introduced into QMS; subsequently, the separated fractions were analyzed by fluorescent microscopy. The separation results portray a successful label-less magnetic separation of the two populations.

[4]To whom correspondence should be addressed. monica.venere@osumc.edu, chalmers.1@osu.edu.
[1]Kyoung-Joo Jenny Park and James Kim contributed equally to this work.
[2]Monica Venere and Jeffrey J. Chalmers contributed equally to this work.
[3]Present address: Arcturus Therapeutics, Inc., San Diego, CA 92121

Conflict of Interest

The authors have no conflict of interest

Keywords

Ferritin; Glioblastoma; Magnetic Susceptibility; Single Cell Magnetophoresis; Iron Metabolism; Stem-like Cells

INTRODUCTION

Iron is an essential mineral and plays a major role in numerous cellular activities in all living cells.(Abbaspour et al., 2014) To briefly summarize its functions, iron atoms are directly and indirectly used in oxygen transport, electron transport, oxidation-reduction reactions, respiratory functions, DNA synthesis, replication, and modification, cell cycle regulation, proliferation and growth, and immune responses.(Abbaspour et al., 2014; Johnson and Wessling-Resnick, 2012; Torti and Torti, 2013; Weiss, 2002; Zhang and Zhang, 2015) Iron is most often observed within the cell in ferrous (Fe^{2+}) or ferric (Fe^{3+}) form. However, when the cells convert free Fe^{2+} to storable Fe^{3+}, the Fenton reaction can occur, producing highly reactive oxygen species (ROS). Because ROS can irreversibly damage DNA, lipids, and proteins, iron levels are tightly regulated through a number of different mechanisms.(Kell and Pretorius, 2014; Pham-Huy et al., 2008; Schieber and Chandel, 2014; Uttara et al., 2009) Furthermore, accumulation of ROS can lead to ferroptosis, an iron-dependent cell death, which again emphasizes the importance of tight control of intracellular iron levels. (Dixon et al., 2012)

As vital as iron is to normal cells, tumorous cells reprogram iron metabolism and adapt different pathways to utilize iron for cancer initiation, growth, metastasis, and survival. Specifically, studies have shown upregulation of critical proteins in the regulation of iron homeostasis, such as transferrin receptor 1 (TfR1) and ferritin, and downregulation of the iron efflux transporter, ferroportin (FPN), in cancer cells.(Torti and Torti, 2013; Zhang and Zhang, 2015) Breast cancer patients whose tumors had low levels of TfR1 and high expression of FPN with decreased levels of hepcidin, a negative regulator of FPN, had a favorable prognostic outcome.(Miller et al., 2011; Pinnix et al., 2010) In pancreatic cancer, iron chelators were shown to inhibit epithelial-mesenchymal transition (EMT) and suppress metastasis.(Richardson et al., 2013) On the other hand, increased ferritin levels in metastatic melanoma promoted cell growth while gaining resistance to oxidative stress with higher metastatic potential.(Torti and Torti, 2013) Taken together, the body of data demonstrates that dysregulated iron metabolism is selected in cancer cells. However, there are a considerable amount of studies with conflicting outcomes, emphasizing the complexity and heterogeneity of cancer.(Crielaard et al., 2017) In fact, the product of the Fenton reaction, ROS, can also contribute to both tumor promotion and inhibition as it can be toxic (oxidative stress) and beneficial (redox signaling).(Basuli et al., 2017; Crielaard et al., 2017)

More recently, further diversity in the regulation of iron metabolism has been noted within the same tumor (intratumoral heterogeneity). It has been demonstrated in glioblastoma (GBM) that self-renewing stem-like cells scavenge iron more effectively than other tumor cells via elevated levels of TfR and ferritin.(Schonberg et al., 2015) As a result, GBM cancer stem-like cells (CSCs) had 2- to 3-fold higher iron uptake compared to the matched non-

stem tumor cells (NSTCs), and knockdown of ferritin mRNA suppressed the growth and tumor-initiating ability of CSCs.(Basuli et al., 2017) Increased intracellular iron has since been validated for breast and lung CSCs.(Chanvorachote and Luanpitpong, 2016; Conti et al., 2016) This presents the possibility to use these differences in the regulation of iron metabolism between CSCs and NSTCs as an intrinsic, label-free method to separate these two cell populations.

Single Cell Magnetophoresis (SCM) is an instrument, previously developed and reported as Cell Tracking Velocimetry (CTV), that can measure magnetic susceptibility of individual cells.(Chalmers et al., 1999; Chalmers et al., 2017; McCloskey et al., 2003; Zborowski et al., 2003) Through a square glass channel, cell suspensions are flowed through a magnetic field with nearly constant and well-characterized magnetic energy gradient (S_m) of 365 T*A/mm^2. The SCM software is then triggered to track the horizontal and vertical movements of on the order of one hundred to one thousand cells within the region of interest (ROI). The horizontal component (u_m; magnetic velocity) of the cell movement is solely driven by the magnetic field, while the vertical component describes the settling velocity (u_s) affected by the gravitational force, g:

$$u_m = \frac{(\chi_{Cell} - \chi_{Fluid})V_{Cell}}{3\pi D_{Cell}\eta} S_m \quad (1)$$

$$u_s = \frac{(\rho_{Cell} - \rho_{Fluid})V_{Cell}}{3\pi D_{Cell}\eta} g \quad (2)$$

In the above equations, χ_{Cell} and χ_{Fluid} are the magnetic susceptibilities of the cell and fluid respectively, V_{Cell} is the volume of the cell, D_{Cell} is the hydrodynamic diameter of the cell, η is the viscosity of the suspending fluid, and ρ_{Cell} and ρ_{Fluid} are the mass densities of the cell and fluid, respectively. When Equation 1 is divided by Equation 2, one obtains:

$$\frac{u_m}{u_s} = \frac{(\chi_{Cell} - \chi_{Fluid})S_m}{(\rho_{Cell} - \rho_{Fluid})g} \quad (3)$$

Note this ratio is no longer a function of the size (volume and diameter) of the cell nor the fluid viscosity; correspondingly the magnetic susceptibility of the cell is only a function of the cell's magnetic susceptibility and density. Further re-arranging leads to:

$$\chi_{cell} = \left(\frac{u_m}{u_s}\right)\left(\frac{g}{S_m}\right)\Delta\rho + \quad \chi_{fluid} = \sum \phi_i \chi_i = \phi_{H2O}\chi_{H2O} + \phi_{biomass}\chi_{biomass} + \quad (4)$$

$$\phi_{Fe2+}\chi_{Fe2+} + \phi_{Fe3+}\chi_{Fe3+} + \quad \phi_{ferritin}\chi_{ferritin}$$

As presented in Equation 4, the magnetic susceptibility of a cell is the sum of the magnetic susceptibilities of its constituents where Φ_{H20}, $\Phi_{biomass}$, Φ_{Fe2+}, Φ_{Fe3+}, and $\Phi_{ferritin}$, are the volume fraction of water, biomass, Fe^{2+}, Fe^{3+}, and ferritin within the cell.(Sun et al., 2011; Zborowski et al., 2003) It is fundamentally understood, and experimentally demonstrated, that the magnetic, volumetric susceptibility of biomass, not containing iron, is slightly less than water (-0.905×10^{-5}, SI units).

In contrast, iron ions, Fe^{2+} and Fe^{3+}, have magnetic moments of 4 and 5 Bohr Magnetons (μ_B) respectively.(Dietrich et al., 2017) The iron storage protein, ferritin, can store up to 4,500 Fe^{3+} atoms, but the magnetic moment of "full" ferritin only corresponds to approximately 100 to 400 μ_B.(Brem et al., 2006; García-Prieto et al., 2016) This reduced number of Bohr magnetons, on a per atom basis, is the results of the highly-ordered, pseudo-crystalline mineral core contained within a ferritin complex.(Ueno and Watanabe,)

Magnetic susceptibility and magnetic moments are positively correlated using the following relationship:

$$\chi(\mathrm{SI}) = \frac{N_A \mu_0 \mu_{eff}^2}{3k(T - T_C)} \cdot \frac{\rho}{M_W} \quad (5)$$

where N_A is the Avogadro's number, k is the Boltzmann constant, μ_0 is the magnetic permeability of free space, μ_{eff} is the effective magnetic moment, T_C is the Curie or blocking temperature in kelvin, and M_W is the molecular weight. Assuming that free Fe atoms have an average effective magnetic moment of 4.5 μ_B, the volumetric magnetic susceptibility, χ_{Fe}, becomes 0.015 at 25 °C. (Note, this is assuming that μ_{eff} is a simple function of the number of Bohr magnetons).

Using the above relationships, and experimental studies of fresh and aged human red blood cells (hRBCs), the sensitivity of the SCM instrument has been validated to detect the difference in hemoglobin (Hb) concentration to a resolution of 10^7 Hb molecules per cell, which is equivalent to about 3.7 femtograms of iron per cell.(Chalmers et al., 2017) With respect to cancer cells, we have previously reported on the effect of elevated Fe in the growth media of eight cancer cell lines using the CTV system.(Jin et al., 2012) Out of the eight cell lines tested, two, HeLa and K-562, showed significant magnetophoretic mobility, approaching that of deoxygenated RBCs, in normal growth media. (Chalmers et al., 2017; Jin et al., 2012) Upon medium supplementation with addition of iron, a variety of responses was obtained, from inhibition of growth to normal growth and an approximate 10-fold

increase in magnetophoretic mobility (HeLa).(Jin et al., 2012) Responses in the expression of transferrin receptor and ferritin to changes in media iron concentrations were also reported.(Jin et al., 2012)

In this study, we investigated the difference in iron metabolism in GBM CSCs and NSTCs. After exposing the two populations to an elevated iron environment, cells were harvested, and the magnetic susceptibility and viability of the cells were determined on a per cell basis. The observed differences in magnetophoretic mobility between CSCs and NSTCs suggested that this difference can be exploited as a tool to separate CSCs from NSTCs without any further cell markers. A proof of concept separation is presented to demonstrate this concept.

EXPERIMENTAL SECTION

Cell Culture

GBM tissues were originally obtained from primary human brain tumor patient specimens under approved Institutional Review Board protocols. These specimens were maintained through subcutaneous xenografts in the flanks of immunocompromised mice under approved institutional protocols and conducted in accordance with the NIH Guide for the Care and Use of Laboratory Animals. Xenograft tumors were dissociated to a single cell suspension (Worthington Biochemical) and CSCs were isolated using magnetic-activated cell sorting based on the CD133 epitope (CD133/2-APC, Miltenyi Biotec). NSTCs were passed through two rounds of negative sorting for CD133. All CSCs used in these studies have been previously validated for tumor initiation.(Eyler et al., 2011; Guryanova et al., 2011; Lathia et al., 2010; Li et al., 2009) CSCs and NSTCs were transiently cultured in vitro to achieve the cell numbers needed for the experiments. CSCs were cultured in Neurobasal medium (NBM, Invitrogen) with B27 (without Vitamin A, Invitrogen), 10 ng/ml basic fibroblast growth factor (bFGF), 10 ng/ml epidermal growth factor (EGF), L-glutamine (2 mM; Invitrogen), and sodium pyruvate (1 mM; Invitrogen). To grow CSCs as an adherent monolayer, they were seeded onto GelTrex-coated plates or flasks (Gibco, Invitrogen). NSTCs were cultured in Dulbecco's modified Eagle medium (DMEM) with 10% fetal bovine serum (FBS). Prior to plating for each experiment, the percentage of viable cells was calculated by the Trypan Blue exclusion method. Cells were then split into 6 well plates or 25 cm^2 flasks for subsequent experiments. The next day, the media was replaced with CSC or NSTC media containing 0, 0.5, or 1.5 mg/ml of $Fe(NO_3)_3$ and 4.5 or 45 mg/ml of glucose to analyze the iron uptake of the cells for various culture times of 1, 6, 20, 48, 72, or 96 hours at 37 ºC in 5% CO_2 atmosphere.

Single Cell Magnetophoresis

After cultivation, SCM samples were prepared as reported in previous studies.(Chalmers et al., 1999; Chanvorachote and Luanpitpong, 2016; McCloskey et al., 2003; Zborowski et al., 2003) Cells were detached by TrypLE Express (12604–013, Gibco) and collected in 15 ml centrifuge tubes. After centrifuging at 350 x g for 5 min, supernatants were discarded and 200 ul to 4 ml of new media was added depending on the pellet size. Using the Trypan Blue exclusion method, the numbers of viable and dead cells were counted. Subsequently, Calcein-AM (80011–3, Biotium) in 1:200 was added to the solution and incubated at room

temperature for 30 minutes in dark. After washing, the volume of each sample was adjusted to make the final concentrations to be 10^6 cells/ml in PBS containing 0.1% Pluronic F-68 Non-ionic Surfactant (24040–032, Gibco).

The samples were loaded into the channel as shown in Figure S2. The magnetically induced velocity of cells or particles were measured three times each using fluorescent (only metabolically active Calcein-AM-dyed cells) and dark field (whole sample) filter attached to a CCD camera (Retiga 200R, QImgaing, Canada). Captured images were processed to calculate magnetic susceptibility using an in-house program, and the acquired data were analyzed afterwards.(Moore et al., 2004)

Separation using Quadrupole Magnetic Sorter

Pure populations of GBM CSCs and NSTCs were cultured in iron-enriched media (1.5 mg/ml $Fe(NO_3)_3$), harvested after 20 hrs, and stained separately at room temperature for 30 minutes in dark: CSCs with 10 uM CellTracker Blue CMAC (C2110, Invitrogen) and NSTCs with 10 uM Cell Tracker Red CMTPX (C34552, Invitrogen). Samples were then washed three times by centrifugation at 350 x g for 5 min, followed by decanting the supernatants. The concentration of the cell suspensions was adjusted to 10^6 cells/ml in null media, NBM without any supplements, containing 0.1% Pluronic F-68 solution.

In order to optimize the separation, the magnetic susceptibility calculated from SCM was fed to an in-house program written in Maple to determine the optimal flow rate and ratio for the binary inlet. Sample, buffer, collection and deposit collection tubes were connected as shown in Figure 4A. The samples were run with PBS at specified inlet flow ratio and rate, and the flow rates were controlled by syringe pumps. Subsequently, both the collection and deposit fractions were collected, loaded onto slides, and observed under fluorescent microscope (Nikon Eclipse 80i Advance Research Microscope) for analysis.

Density Measurement

To make a 100% Percoll solution, 9 parts (v/v) of Percoll (GE Healthcare, Piscataway, NJ, USA) was mixed with 1 part (v/v) of 10× concentrated PBS. The 100% Percoll solution was diluted into 5 ml of 40%, 30%, 20%, and 10% Percoll solutions in 1x PBS. Pure 1x PBS was used as 0% Percoll solution. 2 mL of the 40% Percoll gradient solution was layered at the bottom of the 15 ml Falcon tube, and the rest of the 30%, 20%, 10% and 0% percoll solutions (2 ml each) were added at a 45-degree angle with care not to disturb the layers. The density markers beads (GE Healthcare, Piscataway, NJ, USA) and CSCs and NSTCs incubated at 24 hours at normal media and 1.5 mg/ml $Fe(NO_3)_3$ were each suspended in cold 20% Percoll solution, added to the top of the Percoll gradient tubes, and centrifuged for 15 minutes at 800 x g. After centrifugation, the visible heights of the cells and the density marker beads were compared for calculation of the density of the cells.

RESULTS AND DISCUSSION

To facilitate iron uptake in cells, screening studies were conducted on GBM CSCs and NSTCs with elevated iron.(Jin et al., 2012) We varied glucose concentration in the culture media because higher glucose uptake was identified as one of the key distinctions between

GBM CSCs and NSTCs as well as many other cancer cells.(Antoch et al., 2003; DeBerardinis et al., 2008; Flavahan et al., 2013; Fong et al., 2015; Vander Heiden et al., 2009; Jin et al., 2012) As summarized in Table 1, two different concentrations of ferric nitrate, $Fe(NO_3)_3$, 2.1 and 6.2 mM (0.5 and 1.5 mg/mL) and two concentrations of glucose, 1x and 10x (glucose level relative to the amount that is already in the media) were screened.

SCM Analysis of CSCs and NSTCs

Initial screening studies of CSCs and NSTCs indicated that elevated glucose did not have any effect, by itself, in increasing the magnetic susceptibility of GBM cells (Figure S1). However, elevated iron did. Figures 1A and 1B present representative scatter plots of the experimentally measured, magnetic velocity versus the settling velocity for the CSCs and NSTCs cultured in the highest concentration of Fe-supplemented media (each dot corresponds to a single tracked cell). The current construction/operation of the SCM instrument requires that one chooses the filter set/optical setting for a given experiment. Consequently, two sets of experiments were conducted on each cell suspension: a) the use of dark field optics, DF, which allows all cells to be tracked, and b) a fluorescent filter set, FL, compatible with the viability stain, Calcein-AM. Therefore, DF corresponds to all cells present while FL corresponds to fluorescent, and presumably viable, cells. A number of striking observation can be made in Figures 1A and 1B; the CSCs are significantly less magnetic than the NSTCs, and the distribution of the magnetic NSTCs is significantly greater. A closer examination indicates that most of these magnetic, NSTCs only appear as DF images and not FL images; implying they are non-viable.

To allow a more quantitative and statistical comparison, the experimentally measured magnetic velocity was divided by settling velocity for each tracked cell, as mathematically presented in Equation 3 above (Figures 1C and 1D). This ratio of the experimental data for each tracked cell allows a mean and 95% confidence interval to be calculated for each experimental condition that is only a function of the cell's magnetic susceptibility and density.

In normal media (condition #1 in Figures 1C and 1D), both CSCs and NSTCs exhibit diamagnetic behavior suggested by the small negative ratios. This is expected as discussed above in Equation 5 and observed in previous studies of a variety of cell types.(Chalmers et al., 2010; Chalmers et al., 2017; Chosy et al., 2003; Sun et al., 2011) In contrast, as the iron concentration in the culture media increased (media conditions #2 and #3), the average u_m/u_s ratios increased for both CSCs and NSTCs, with the largest changes, relative to the normal media, for the NSTCs. While the differences in the mean values of the u_m/u_s ratio between the cells tracked with the fluorescence optics (the viable cells) compared to all tracked cells (dark field optics) with the CSCs are within the 95% confidence interval, thereby implying no change (Figure 1C), a large difference outside the confidence intervals is observed in the highest iron concentration at 40 hours between the CSCs and the NSTCs (Figure 1D). Further, the error bars (95% confidence level) are larger in the NSTCs, which is consistent with the large scatter in the dot plots (Figure 1B compared to 1A).

Viability measurements

Prior to each harvest for SCM measurements, the cells were washed and resuspended in buffer with a fraction of the cells removed for viability measurements with trypan blue. These viability measurements are presented in Figures 1E and 1F. While both types of cells exhibited a slow decrease in viability, there was a slightly lower percent viability in the NSTCs. It is not clear at this time why there appears to be an oscillation in viability. With respect to growth, only the CSCs cultured in conditions #1 and #2 exhibited significant growth after 48 hours (165% and 120% change in number of viable cells respectively) while NSTCs had 10% to 25% reduction in total number of viable cells (data not shown).

Density and Coulter Counter measurements

Given the implication of the data presented in Figure 1 that the uptake of iron results in the increased ratio of u_m/u_s, one might presume that the increased iron content of the cells would also increase the density, and correspondingly affect the ratio of u_m/u_s (Equation 3 indicated that this ratio is proportional to the difference in density of the cell with respect to the suspending buffer). Using percoll density measurement methodology, the densities of four different cell suspensions, in normal medium and high Fe concentrations, for both the CSCs and NSTCs were determined. No trends in the mean density was observed with increasing Fe concentration. The overall mean of all four measurements was 1.03 g/ml, with a standard deviation of 0.015. Since the accuracy of this measurements, at best, is to 3 significant figures, and no significant trends were observed between normal and elevated Fe media, it can be concluded that a change in density cannot account for the observed increase in the ratio of u_m/u_s from 0.3 to over 10 fold (CSCs, media condition #3, to NSTCs, media condition #3). Consistent with no significant change in cell density, the experimentally-determined average settling velocities for all samples was 3.05 um/s and did not show a particular trend with increasing iron concentration.

While it might be expected that CSCs would exhibit a higher magnetic susceptibility than NSTCs, since it was previously reported that CSCs more readily uptake Fe over NSTCs(Schonberg et al., 2015) (discussed above), iron stored in ferritin has a significantly lower magnetic susceptibility, on a per iron atom basis, than free iron atoms. Consequently, two cells can contain the same, absolute number of iron atoms, but if a significant number of these iron atoms are containing within ferritin in one of the cells, then that cell will have a lower magnetic susceptibility than the cell without the ferritin.

To determine the reproducibility of these observations, two different patient samples of CSCs and NSTCs were each tested at least twice. Figure 2 presents these studies. While some variability exists, a clear difference between CSCs and NSTCs is seen in all four studies.

Separation based on Magnetophoretic Mobility

Currently, CSCs are prospectively isolated using cell surface markers (including the CSCs and NSTCs used in this study).(Bao et al., 2006; Venere et al., 2014; Venere et al., 2015) This approach has allowed for the functional validation of tumor initiation for CSCs over the NSTC population from the same tumor in an orthotopic xenograft models.(Bao et al., 2006)

However, surface epitopes have also created great controversy in the CSC field as some groups have demonstrated tumor initiation for both marker positive and negative populations as well as heterogeneity of marker expression based on micro-environmental factors.(Beier et al., 2007; Shmelkov et al., 2008) Another issue with cell surface markers is that for every marker identified to date, their expression can also be seen in normal adult stem cells, embryonic stem cells, or normal tissue.(Kim and Ryu, 2017) The presence of surface epitopes can also be inconsistent due to cell cycle dependent expression as well as receptor recycling.(Jaksch et al., 2008) Relevant to the latter point, the fluorescent or tagged antibodies that are currently used for prospective isolation can drive internalization of surface receptors.(Liao-Chan et al., 2015)

The data presented above support that CSCs can be separated from NSTCs based solely on the magnetic susceptibility differences between the two cell types; i.e. a label-less separation methodology. Figure 3 presents overlapping histograms showing the distributions of CSCs and NSTCs cultured in media supplemented with 1.5 mg/ml Fe (condition #3) for 20 and 48 hours. The x-axis corresponds to the experimentally measured velocity (mm/s), and the second x-axis corresponds to the cell's magnetophoretic mobility, (mm^3*s/kg), calculated by dividing u_m by S_m.

We have previously reported on a flow through, magnetic cell separation system, referred to as the Quadrupole Magnetic Separator, QMS.(Jing et al., 2007; Lara et al., 2004; Moore et al., 2018; Williams et al., 1999) This system is typically operated with two flows in (the cell suspension to be separated, and a buffer, sheath fluid), and either one or two exit flows out. (Lara et al., 2006) Most recently and relevant to this study, the QMS has been used to separate human blood cells, hRBCs, based on their intrinsic magnetic susceptibility.(Moore et al., 2018) Figure 4A presents this QMS system operated with the two flow in and one flow out mode of operation.

Using this QMS system, four proof of concept separations were conducted on mixtures of GBM CSCs and NSTCs, cultured separately in 1.5 mg/ml (6.20 mM) $Fe(NO_3)_3$ for 20 hours. Each harvested cell suspension was then stained with Cell Tracker dyes; CSCs were stained with Cell Tracker Blue, and NSTCs were stained with Cell Tracker Red. Table 2 presents the summary of these four experiments, including initial number of cells, ratio of CSCs to NSTCs, total flow rate through the system, and the final enrichment rate.

Figure 4B presents representative images of slides made of the flow-through collection and the magnetically deposited cells that were washed out of the system after the separation. It was expected to observe some red cells (NSTCs) included in the flow through fraction since there is some overlapping regions between CSCs and NSTCs, as observed in the histograms of Figure 3.

A concern can be raised that the flow through the QMS system can damage cells. We briefly discussed this concern in one of our prior publications, Moore et al. (2018), never the less, an additional analysis will be given here. All the dimensions of the apparatus, from the syringe pump to the final collections tubes are known; from these dimensions, and the known flow rates used, the Reynolds number for all flows is clearly in the laminar flow

regime. In the publication Mollet *et al.* (2004), figures presenting the Energy dissipation rate, for a range of laminar flow geometries, and flow rates, are presented. Further, Chalmers et al. (2015) summarized the current reported levels of EDR that are known to damage cells, including human cancer cells. It is estimated that the maximum EDR value that the GBMs are exposed to in the QMS is 10^4 W/m^3 which is 2 orders of magnitude the levels are which damage begin to be reported. However, estimates of EDR are in typical FACS can easily exceed 10^6 W/m^3 at which cell damage begins to occur (Mollet *et al.* 2008).

Iron concentration and kinetic studies

The previous data confirms that CSCs and NSTCs internalize elevated iron concentrations from the culture media, and that the average magnetic susceptibility of the NSTCs is higher, most likely the result of increased levels of ferritin in the CSCs which can store the iron in less magnetic forms, on a per iron basis. We subsequently investigated the potential of lower concentrations of iron in the incubation media as well as reduced incubation time with respect to increased magnetic susceptibility of CSCs and NSTCs.

In a manner similar to presented above, CSC and NSTC cultures were incubated separately in 0.1, 1.0 and 2.1 mM iron concentrations, and the cells were harvested at 1, 6, 24, and 48 hours. The incubations of both CSCs and NSTCs in 0.1 and 1.0 mM iron produced insufficient changes during the 24 hour period between the elevated iron and the controls for either the CSCs or the NSTCs to allow for the potential of separations. Conversely, the 2.1 mM iron concentration incubations, while insufficient in 24 hours to effect a separation, did exhibit a trend, that when combined with the data presented above, the 2.1 mM iron is a potential Fe incubation concentration for further separation studies (Figure 5).

CONCLUSION

The data presented above clearly demonstrate that elevated Fe in the culture media results in increased magnetic susceptibility of GBM cells, and that a difference between GBM CSCs and NSTCs exists. Further, the method of measurements, the type of data collected, and the mathematical relationships presented indicate this increased magnetic susceptibility of GBM cells is solely the result of increased intracellular iron. Independent of this study, it was previously demonstrated that GBM CSCs uptake higher iron more effectively than the matched NSTCs, consistent with the mechanism that specifically involves higher levels of TfR and ferritin.(Schonberg et al., 2015) While this observation that CSCs take up more Fe than NSTCs, as it was also presented above, on a per Fe atom basis, might lead to thinking that CSCs would be more magnetic than NSTCs, Fe is stored in the pseudo-crystalline mineral core of ferritin which results in each Fe atom only having 20% of the magnetic susceptibility of a free Fe atom. Consequently, while initially counter intuitive, the magnetic susceptibility measurements presented in this contribution are consistent with the work of Schonberg.(Schonberg et al., 2015) One of our future goals will further investigate the correlation between increased iron and glucose metabolisms in tumorous cells as there is a definitive proof of increased glucose and iron composition especially within GBM self-renewing CSCs.(Flavahan et al., 2013; Schonberg et al., 2015)

While the work presented demonstrates the potential to separate CSCs from NSTCs, to further validate our results, separation needs to be performed on unsorted GBM cells and followed by a limited dilution assay to test for self-renewal as well as tumor initiation studies. Limited dilution assays and tumor initiation are both functional assays for CSCs, testing the ability to form tumorspheres from a lowest number of cells (where the NSTCs would not form the tumorsphere) in vitro and self-renewal ability in vivo, respectively. Through these two functional assays, we can characterize the collection and deposit fractions more accurately and conclude whether this technology holds potential benefits in clinical research studying cancer stem cells. Additionally, a comparison of magnetic separation to current methodologies of enriching for CSCs, such as cell surface markers or isolation of the side-population, needs to be addressed. Finally, utilizing dysregulated iron metabolism unique to CSCs, various innovative mechanisms can be developed to target CSCs in cancer patients.

Supplementary Material

Refer to Web version on PubMed Central for supplementary material.

ACKNOWLDEDGEMENT

This work was supported in part by the Ohio State University Comprehensive Cancer Center, the American Cancer Society (RSG-18-066-01-TBG), and the National Heart, Lung, and Blood Institute (1R01HL131720-01A1)

REFERENCES

Abbaspour N, Hurrell R, Kelishadi R. 2014 Review on iron and its importance for human health. J. Res. Med. Sci 19:164–74. http://www.ncbi.nlm.nih.gov/pubmed/24778671. [PubMed: 24778671]

Antoch G, Vogt FM, Freudenberg LS, Nazaradeh F, Goehde SC, Barkhausen J, Dahmen G, Bockisch A, Debatin JF, Ruehm SG. 2003 Whole-Body Dual-Modality PET/CT and Whole-Body MRI for Tumor Staging in Oncology. JAMA 290:3199 http://www.ncbi.nlm.nih.gov/pubmed/14693872. [PubMed: 14693872]

Bao S, Wu Q, McLendon RE, Hao Y, Shi Q, Hjelmeland AB, Dewhirst MW, Bigner DD, Rich JN. 2006 Glioma stem cells promote radioresistance by preferential activation of the DNA damage response. Nature 444:756–760. http://www.ncbi.nlm.nih.gov/pubmed/17051156. [PubMed: 17051156]

Basuli D, Tesfay L, Deng Z, Paul B, Yamamoto Y, Ning G, Xian W, McKeon F, Lynch M, Crum CP, Hegde P, Brewer M, Wang X, Miller LD, Dyment N, Torti FM, Torti SV. 2017 Iron addiction: a novel therapeutic target in ovarian cancer. Oncogene 36:4089–4099. http://www.ncbi.nlm.nih.gov/pubmed/28319068. [PubMed: 28319068]

Beier D, Hau P, Proescholdt M, Lohmeier A, Wischhusen J, Oefner PJ, Aigner L, Brawanski A, Bogdahn U, Beier CP. 2007 CD133+ and CD133- Glioblastoma-Derived Cancer Stem Cells Show Differential Growth Characteristics and Molecular Profiles. Cancer Res 67:4010–4015. http://www.ncbi.nlm.nih.gov/pubmed/17483311. [PubMed: 17483311]

Brem F, Stamm G, Hirt AM. 2006 Modeling the magnetic behavior of horse spleen ferritin with a two-phase core structure. J. Appl. Phys 99:123906 http://aip.scitation.org/doi/10.1063/1.2206101.

Chalmers JJ, 2015 Mixing, aeration and cell damage, 30+ years later: what we learned, how it affected the cell culture industry, and and what we would like to know more about. Current Opinions in Chemical Engineering 10:94–102.

Chalmers JJ, Jin X, Palmer AF, Yazer MH, Moore L, Amaya P, Park K, Pan X, Zborowski M. 2017 Femtogram Resolution of Iron Content on a Per Cell Basis: Ex Vivo Storage of Human Red Blood

Cells Leads to Loss of Hemoglobin. Anal. Chem 89:3702–3709. http://www.ncbi.nlm.nih.gov/pubmed/28230974. [PubMed: 28230974]

Chalmers JJ, Xiong Y, Jin X, Shao M, Tong X, Farag S, Zborowski M. 2010 Quantification of non-specific binding of magnetic micro- and nanoparticles using cell tracking velocimetry: Implication for magnetic cell separation and detection. Biotechnol. Bioeng 105:1078–93. http://www.ncbi.nlm.nih.gov/pubmed/20014141. [PubMed: 20014141]

Chalmers JJ, Haam S, Zhao Y, McCloskey K, Moore L, Zborowski M, Williams PS. 1999 Quantification of cellular properties from external fields and resulting induced velocity: Magnetic susceptibility. Biotechnol. Bioeng 64:519–526. http://doi.wiley.com/10.1002/%28SICI%291097-0290%2819990905%2964%3A5%3C519%3A%3AAID-BIT2%3E3.0.CO%3B2-V. [PubMed: 10404232]

Chanvorachote P, Luanpitpong S. 2016 Iron induces cancer stem cells and aggressive phenotypes in human lung cancer cells. Am. J. Physiol. Physiol 310:C728–C739. http://www.ncbi.nlm.nih.gov/pubmed/26911281.

Chosy EJ, Nakamura M, Melnik K, Comella K, Lasky LC, Zborowski M, Chalmers JJ. 2003 Characterization of antibody binding to three cancer-related antigens using flow cytometry and cell tracking velocimetry. Biotechnol. Bioeng 82:340–351. http://www.ncbi.nlm.nih.gov/pubmed/12599261. [PubMed: 12599261]

Conti L, Lanzardo S, Ruiu R, Cadenazzi M, Cavallo F, Aime S, Crich SG. 2016 L-Ferritin targets breast cancer stem cells and delivers therapeutic and imaging agents. Oncotarget 7:66713–66727. http://www.ncbi.nlm.nih.gov/pubmed/27579532. [PubMed: 27579532]

Crielaard BJ, Lammers T, Rivella S. 2017 Targeting iron metabolism in drug discovery and delivery. Nat. Rev. Drug Discov 16:400–423. http://www.ncbi.nlm.nih.gov/pubmed/28154410. [PubMed: 28154410]

DeBerardinis RJ, Lum JJ, Hatzivassiliou G, Thompson CB. 2008 The Biology of Cancer: Metabolic Reprogramming Fuels Cell Growth and Proliferation. Cell Metab 7:11–20. http://www.ncbi.nlm.nih.gov/pubmed/18177721. [PubMed: 18177721]

Dietrich O, Levin J, Ahmadi S-A, Plate A, Reiser MF, Bötzel K, Giese A, Ertl-Wagner B. 2017 MR imaging differentiation of Fe2+ and Fe3+ based on relaxation and magnetic susceptibility properties. Neuroradiology 59:403–409. http://www.ncbi.nlm.nih.gov/pubmed/28324122. [PubMed: 28324122]

Dixon SJ, Lemberg KM, Lamprecht MR, Skouta R, Zaitsev EM, Gleason CE, Patel DN, Bauer AJ, Cantley AM, Yang WS, Morrison B, Stockwell BR. 2012 Ferroptosis: An Iron-Dependent Form of Nonapoptotic Cell Death. Cell 149:1060–1072. http://www.ncbi.nlm.nih.gov/pubmed/22632970. [PubMed: 22632970]

Eyler CE, Wu Q, Yan K, MacSwords JM, Chandler-Militello D, Misuraca KL, Lathia JD, Forrester MT, Lee J, Stamler JS, Goldman SA, Bredel M, McLendon RE, Sloan AE, Hjelmeland AB, Rich JN. 2011 Glioma Stem Cell Proliferation and Tumor Growth Are Promoted by Nitric Oxide Synthase-2. Cell 146:53–66. http://www.ncbi.nlm.nih.gov/pubmed/21729780. [PubMed: 21729780]

Flavahan WA, Wu Q, Hitomi M, Rahim N, Kim Y, Sloan AE, Weil RJ, Nakano I, Sarkaria JN, Stringer BW, Day BW, Li M, Lathia JD, Rich JN, Hjelmeland AB. 2013 Brain tumor initiating cells adapt to restricted nutrition through preferential glucose uptake. Nat. Neurosci 16:1373–82. http://www.ncbi.nlm.nih.gov/pubmed/23995067. [PubMed: 23995067]

Fong MY, Zhou W, Liu L, Alontaga AY, Chandra M, Ashby J, Chow A, O'Connor STF, Li S, Chin AR, Somlo G, Palomares M, Li Z, Tremblay JR, Tsuyada A, Sun G, Reid MA, Wu X, Swiderski P, Ren X, Shi Y, Kong M, Zhong W, Chen Y, Wang SE. 2015 Breast-cancer-secreted miR-122 reprograms glucose metabolism in premetastatic niche to promote metastasis. Nat. Cell Biol 17:183–194. http://www.ncbi.nlm.nih.gov/pubmed/25621950. [PubMed: 25621950]

García-Prieto A, Alonso J, Muñoz D, Marcano L, Abad Díaz de Cerio A, Fernández de Luis R, Orue I, Mathon O, Muela A, Fdez-Gubieda ML 2016 On the mineral core of ferritin-like proteins: structural and magnetic characterization. Nanoscale 8:1088–1099. http://xlink.rsc.org/?DOI=C5NR04446D. [PubMed: 26666195]

Guryanova OA, Wu Q, Cheng L, Lathia JD, Huang Z, Yang J, MacSwords J, Eyler CE, McLendon RE, Heddleston JM, Shou W, Hambardzumyan D, Lee J, Hjelmeland AB, Sloan AE, Bredel M, Stark

GR, Rich JN, Bao S. 2011 Nonreceptor Tyrosine Kinase BMX Maintains Self-Renewal and Tumorigenic Potential of Glioblastoma Stem Cells by Activating STAT3. Cancer Cell 19:498–511. http://www.ncbi.nlm.nih.gov/pubmed/21481791. [PubMed: 21481791]

Vander Heiden MG, Cantley LC, Thompson CB. 2009 Understanding the Warburg Effect: The Metabolic Requirements of Cell Proliferation. Science (80-.) 324:1029–1033. http://www.ncbi.nlm.nih.gov/pubmed/19460998.

Jaksch M, Munera J, Bajpai R, Terskikh A, Oshima RG. 2008 Cell Cycle-Dependent Variation of a CD133 Epitope in Human Embryonic Stem Cell, Colon Cancer, and Melanoma Cell Lines. Cancer Res 68:7882–7886. http://www.ncbi.nlm.nih.gov/pubmed/18829544. [PubMed: 18829544]

Jin X, Chalmers JJ, Zborowski M. 2012 Iron Transport in Cancer Cell Culture Suspensions Measured by Cell Magnetophoresis. Anal. Chem 84:4520–4526. http://pubs.acs.org/doi/10.1021/ac3004677. [PubMed: 22500468]

Jing Y, Moore LR, Williams PS, Chalmers JJ, Farag SS, Bolwell B, Zborowski M. 2007 Blood progenitor cell separation from clinical leukapheresis product by magnetic nanoparticle binding and magnetophoresis. Biotechnol. Bioeng 96:1139–1154. http://www.ncbi.nlm.nih.gov/pubmed/17009321. [PubMed: 17009321]

Johnson EE, Wessling-Resnick M. 2012 Iron metabolism and the innate immune response to infection. Microbes Infect 14:207–216. http://www.ncbi.nlm.nih.gov/pubmed/22033148. [PubMed: 22033148]

Kell DB, Pretorius E. 2014 Serum ferritin is an important inflammatory disease marker, as it is mainly a leakage product from damaged cells. Metallomics 6:748–73. http://www.ncbi.nlm.nih.gov/pubmed/24549403. [PubMed: 24549403]

Kim W-T, Ryu CJ. 2017 Cancer stem cell surface markers on normal stem cells. BMB Rep 50:285–298. http://www.ncbi.nlm.nih.gov/pubmed/28270302. [PubMed: 28270302]

Lara O, Tong X, Zborowski M, Chalmers JJ. 2004 Enrichment of rare cancer cells through depletion of normal cells using density and flow-through, immunomagnetic cell separation. Exp. Hematol 32:891–904. http://www.ncbi.nlm.nih.gov/pubmed/15504544. [PubMed: 15504544]

Lara O, Tong X, Zborowski M, Farag SS, Chalmers JJ. 2006 Comparison of two immunomagnetic separation technologies to deplete T cells from human blood samples. Biotechnol. Bioeng 94:66–80. http://www.ncbi.nlm.nih.gov/pubmed/16518837. [PubMed: 16518837]

Lathia JD, Gallagher J, Heddleston JM, Wang J, Eyler CE, MacSwords J, Wu Q, Vasanji A, McLendon RE, Hjelmeland AB, Rich JN. 2010 Integrin Alpha 6 Regulates Glioblastoma Stem Cells. Cell Stem Cell 6:421–432. http://www.ncbi.nlm.nih.gov/pubmed/20452317. [PubMed: 20452317]

Li Z, Bao S, Wu Q, Wang H, Eyler C, Sathornsumetee S, Shi Q, Cao Y, Lathia J, McLendon RE, Hjelmeland AB, Rich JN. 2009 Hypoxia-Inducible Factors Regulate Tumorigenic Capacity of Glioma Stem Cells. Cancer Cell 15:501–513. http://www.ncbi.nlm.nih.gov/pubmed/19477429. [PubMed: 19477429]

Liao-Chan S, Daine-Matsuoka B, Heald N, Wong T, Lin T, Cai AG, Lai M, D'Alessio JA, Theunissen J-W. 2015 Quantitative Assessment of Antibody Internalization with Novel Monoclonal Antibodies against Alexa Fluorophores. Ed. Sabato D'Auria. PLoS One 10:e0124708 http://dx.plos.org/10.1371/journal.pone.0124708. [PubMed: 25894652]

McCloskey KE, Chalmers JJ, Zborowski M. 2003 Magnetic Cell Separation: Characterization of Magnetophoretic Mobility. Anal. Chem 75:6868–6874. http://www.ncbi.nlm.nih.gov/pubmed/14670047. [PubMed: 14670047]

Miller LD, Coffman LG, Chou JW, Black MA, Bergh J, D'Agostino R, Torti S V, Torti FM, Torti FM. 2011 An iron regulatory gene signature predicts outcome in breast cancer. Cancer Res 71:6728–37. http://www.ncbi.nlm.nih.gov/pubmed/21875943. [PubMed: 21875943]

Mollet M, Ma N, Zhao Y, Brodkey R Taticek R, Chalmers JJ 2004 Bioprcoess Equipment: Characterization of Energy Dissipation Rate and its Potential to Damage Cells. Biotechnol. Prog 20:1437–1448. [PubMed: 15458328]

Mollet M, Godoy-Silva R, Berdugo C, Chalmers JJ 2008 Computer Simulations of the Energy Dissipation Rate in a Fluorescence Activated Cell Sorter: Implications to Cells. Biotechnol. Bioeng 100:260–272. [PubMed: 18078288]

Moore LR, Milliron S, Williams PS, Chalmers JJ, Margel S, Zborowski M. 2004 Control of Magnetophoretic Mobility by Susceptibility-Modified Solutions As Evaluated by Cell Tracking Velocimetry and Continuous Magnetic Sorting. Anal. Chem 76:3899–3907. http://www.ncbi.nlm.nih.gov/pubmed/15253623. [PubMed: 15253623]

Moore LR, Mizutani D, Tanaka T, Buck A, Yazer M, Zborowski M, Chalmers JJ. 2018 Continuous, intrinsic magnetic depletion of erythrocytes from whole blood with a quadrupole magnet and annular flow channel; pilot scale study. Biotechnol. Bioeng 115:1521–1530. http://www.ncbi.nlm.nih.gov/pubmed/29476625. [PubMed: 29476625]

Pham-Huy LA, He H, Pham-Huy C. 2008 Free radicals, antioxidants in disease and health. Int. J. Biomed. Sci 4:89–96. http://www.ncbi.nlm.nih.gov/pubmed/23675073. [PubMed: 23675073]

Pinnix ZK, Miller LD, Wang W, D'Agostino R, Kute T, Willingham MC, Hatcher H, Tesfay L, Sui G, Di X, Torti SV., Torti FM 2010 Ferroportin and Iron Regulation in Breast Cancer Progression and Prognosis. Sci. Transl. Med 2:43ra56–43ra56. http://www.ncbi.nlm.nih.gov/pubmed/20686179.

Richardson A, Kovacevic Z, Richardson DR. 2013 Iron chelation: inhibition of key signaling pathways in the induction of the epithelial mesenchymal transition in pancreatic cancer and other tumors. Crit. Rev. Oncog 18:409–34. http://www.ncbi.nlm.nih.gov/pubmed/23879587. [PubMed: 23879587]

Schieber M, Chandel NS. 2014 ROS Function in Redox Signaling and Oxidative Stress. Curr. Biol 24:R453–R462. http://www.ncbi.nlm.nih.gov/pubmed/24845678. [PubMed: 24845678]

Schonberg DL, Miller TE, Wu Q, Flavahan WA, Das NK, Hale JS, Hubert CG, Mack SC, Jarrar AM, Karl RT, Rosager AM, Nixon AM, Tesar PJ, Hamerlik P, Kristensen BW, Horbinski C, Connor JR, Fox PL, Lathia JD, Rich JN. 2015 Preferential Iron Trafficking Characterizes Glioblastoma Stem-like Cells. Cancer Cell 28:441–455. http://www.ncbi.nlm.nih.gov/pubmed/26461092. [PubMed: 26461092]

Shmelkov SV, Butler JM, Hooper AT, Hormigo A, Kushner J, Milde T, Clair R St., Baljevic M, White I, Jin DK, Chadburn A, Murphy AJ, Valenzuela DM, Gale NW, Thurston G, Yancopoulos GD, D'Angelica M, Kemeny N, Lyden D, Rafii S 2008 CD133 expression is not restricted to stem cells, and both CD133+ and CD133– metastatic colon cancer cells initiate tumors. J. Clin. Invest 118:2111–20. http://www.ncbi.nlm.nih.gov/pubmed/18497886. [PubMed: 18497886]

Sun J, Zborowski M, Chalmers JJ. 2011 Quantification of both the presence, and oxidation state, of Mn in Bacillus atrophaeus spores and its imparting of magnetic susceptibility to the spores. Biotechnol. Bioeng 108:1119–1129. http://www.ncbi.nlm.nih.gov/pubmed/21449026. [PubMed: 21449026]

Torti SV, Torti FM 2013 Iron and cancer: more ore to be mined. Nat. Rev. Cancer 13:342–355. http://www.ncbi.nlm.nih.gov/pubmed/23594855. [PubMed: 23594855]

Ueno T, Watanabe Y. Coordination chemistry in protein cages principles, design, and applications https://www.wiley.com/en-us/Coordination+Chemistry+in+Protein+Cages%3A+Principles%2C+Design%2C+and+Applications-p-9781118078570.

Uttara B, Singh AV, Zamboni P, Mahajan RT. 2009 Oxidative stress and neurodegenerative diseases: a review of upstream and downstream antioxidant therapeutic options. Curr. Neuropharmacol 7:65–74. http://www.ncbi.nlm.nih.gov/pubmed/19721819. [PubMed: 19721819]

Venere M, Hamerlik P, Wu Q, Rasmussen RD, Song LA, Vasanji A, Tenley N, Flavahan WA, Hjelmeland AB, Bartek J, Rich JN. 2014 Therapeutic targeting of constitutive PARP activation compromises stem cell phenotype and survival of glioblastoma-initiating cells. Cell Death Differ 21:258–269. http://www.ncbi.nlm.nih.gov/pubmed/24121277. [PubMed: 24121277]

Venere M, Horbinski C, Crish JF, Jin X, Vasanji A, Major J, Burrows AC, Chang C, Prokop J, Wu Q, Sims PA, Canoll P, Summers MK, Rosenfeld SS, Rich JN. 2015 The mitotic kinesin KIF11 is a driver of invasion, proliferation, and self-renewal in glioblastoma. Sci. Transl. Med 7:304ra143–304ra143. http://www.ncbi.nlm.nih.gov/pubmed/26355032.

Weiss G 2002 Iron and immunity: a double-edged sword. Eur. J. Clin. Invest 32 Suppl 1:70–8. http://www.ncbi.nlm.nih.gov/pubmed/11886435. [PubMed: 11886435]

Williams PS, Zborowski M, Chalmers JJ. 1999 Flow rate optimization for the quadrupole magnetic cell sorter. Anal. Chem 71:3799–807. http://www.ncbi.nlm.nih.gov/pubmed/10489528. [PubMed: 10489528]

Xue W 2016 Measurements of Cellular Intrinsic Magnetism with Cell Tracking Velocimetry and Separation with Magnetic; Ohio State University https://etd.ohiolink.edu/!etd.send_file?accession=osu1461231847&disposition=inline.

Zborowski M, Ostera GR, Moore LR, Milliron S, Chalmers JJ, Schechter AN. 2003 Red blood cell magnetophoresis. Biophys. J 84:2638–45. http://www.ncbi.nlm.nih.gov/pubmed/12668472. [PubMed: 12668472]

Zhang C, Zhang F. 2015 Iron homeostasis and tumorigenesis: molecular mechanisms and therapeutic opportunities. Protein Cell 6:88–100. http://www.ncbi.nlm.nih.gov/pubmed/25476483. [PubMed: 25476483]

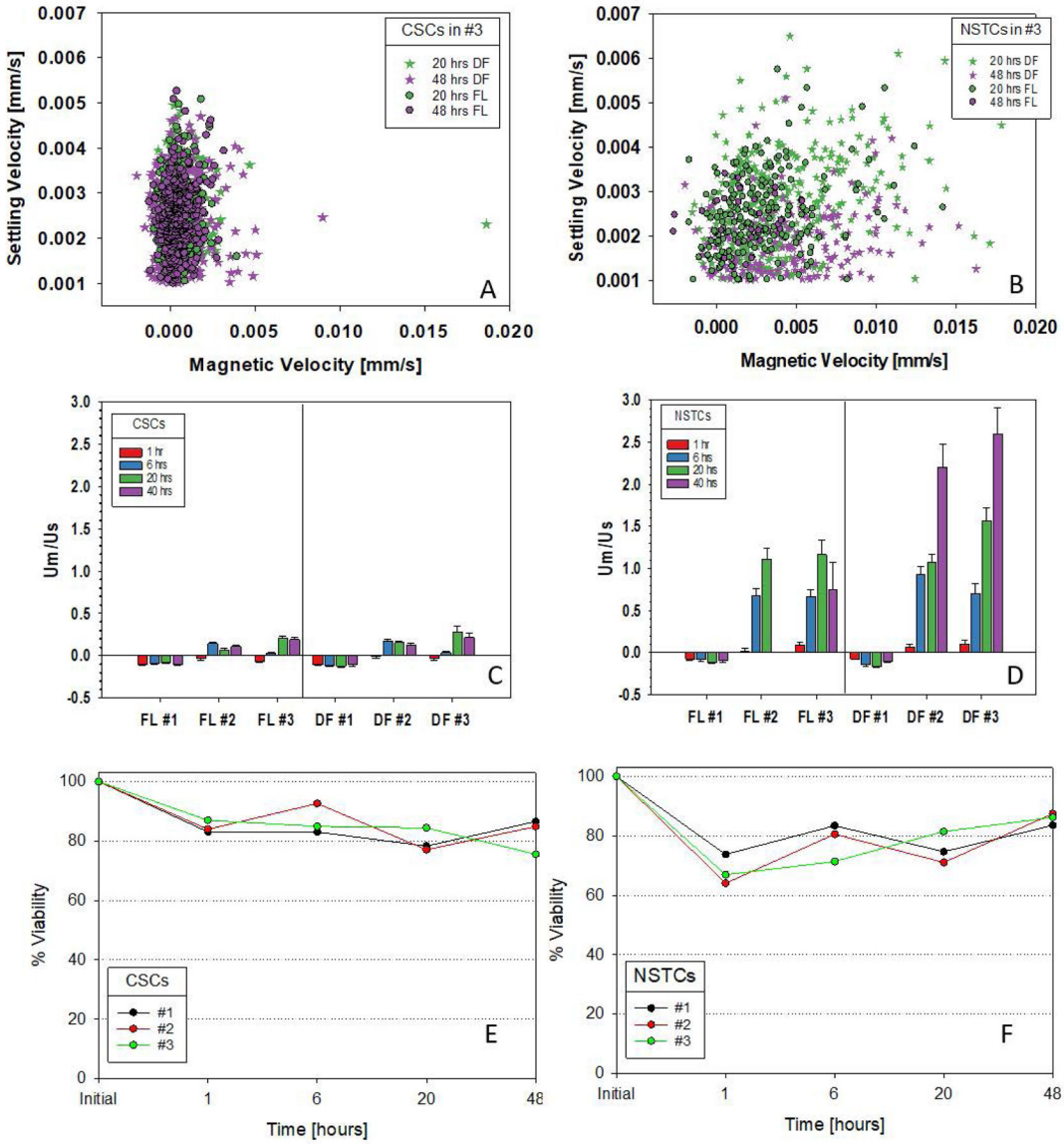

Fig. 1.

Scatter plots, settling velocity vs. magnetic velocity, of CSCs and NSTCs cultured in 6.2 mM Fe for 20 and 48 hours: 1A and 1B. The DF and FL abbreviations correspond to dark field optics and fluorescence optics, respectively. Ratio of magnetic to settling velocity for CSCs and NSTCs at 1, 6, 20 and 40 hours of incubation in three different Fe concentrations, designated 1, 2, 3, which correspond to normal media, 2.1 and 6.2 mM Fe: Figures 1C and 1D. Error bars correspond to one standard deviation. Percent of cell population that is viable, CSCs and NSTC, as function of time, for each of the three Fe concentrations: 1E and 1F.

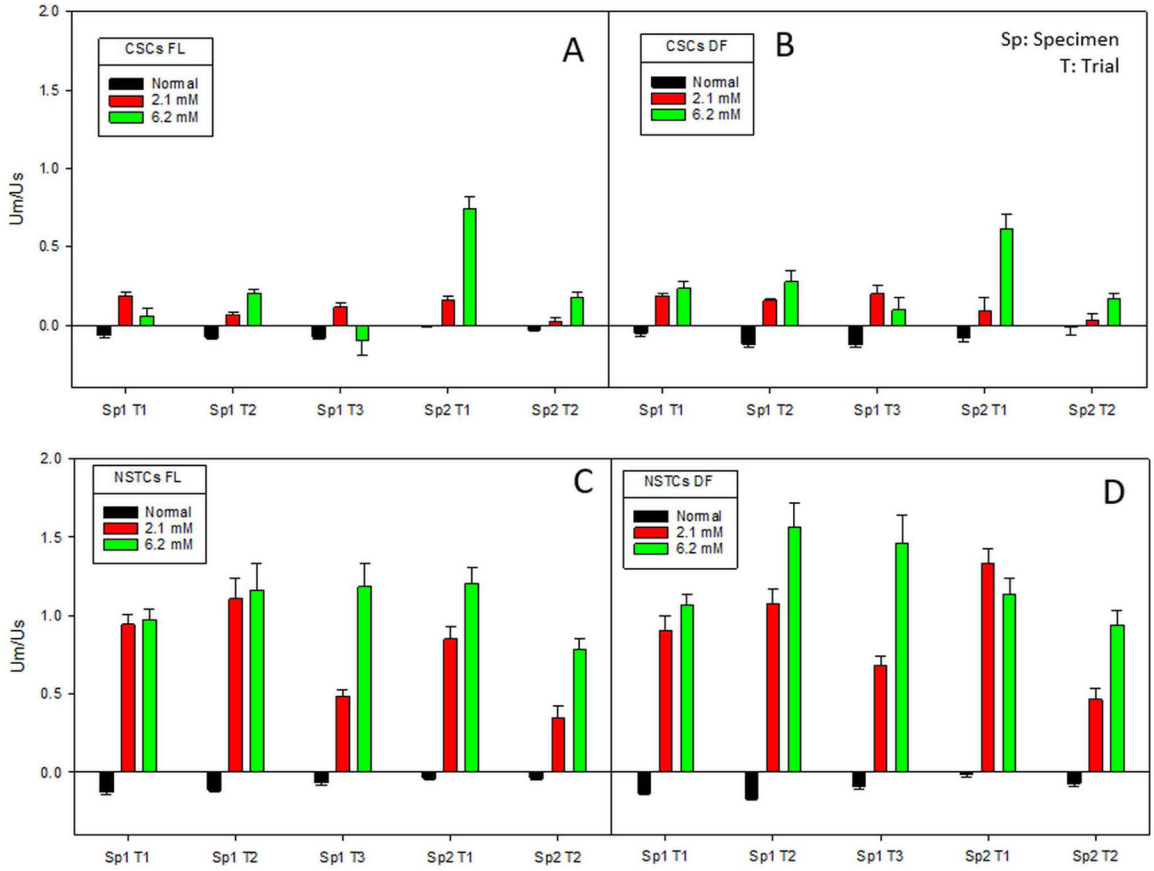

Fig. 2.

Ratio of magnetic to settling velocity for CSCs, 2A and 2B, and NSTCs, 2C and 2D, in normal, 2.1 mM and 6.2 mM Fe after 24 hours of incubation. 2A and 2C correspond to fluoresce optics, and 2B and 2D correspond to dark field optics.

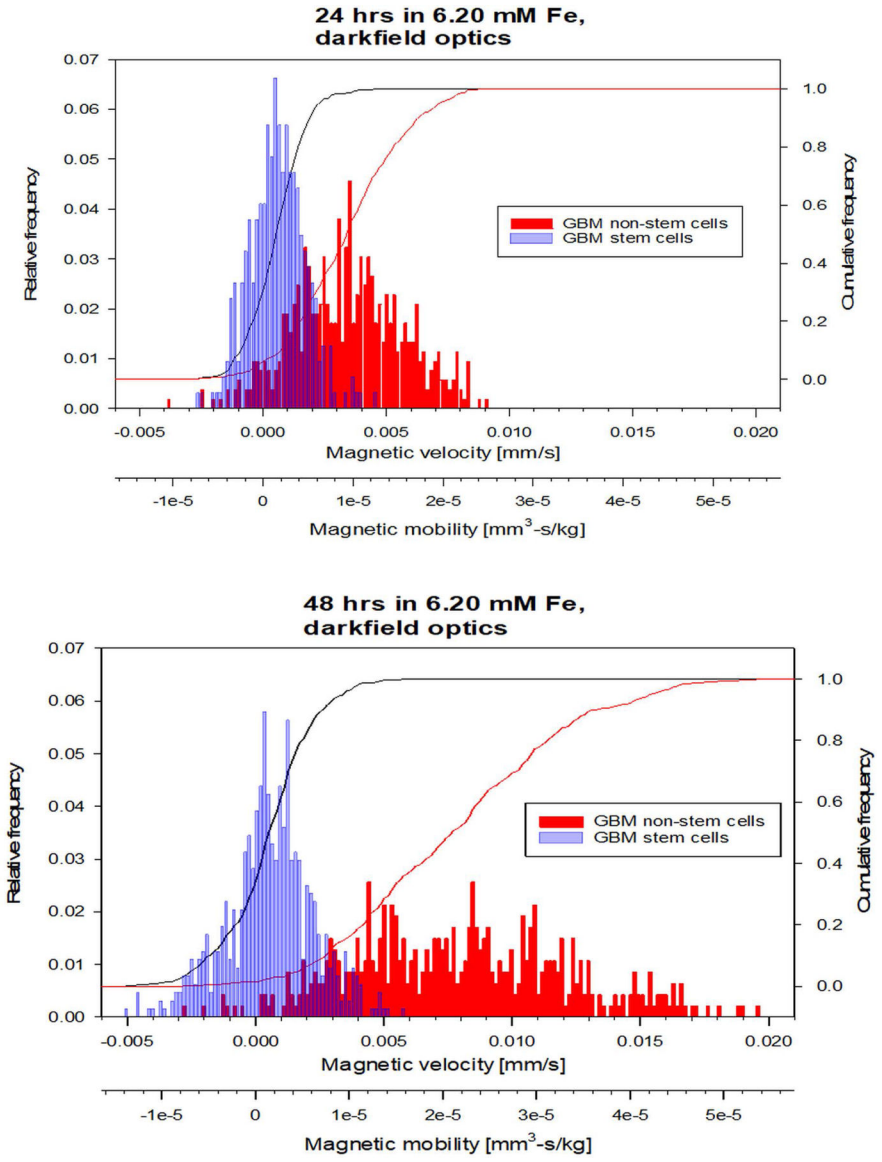

Fig. 3.

Histograms of the magnetic velocity and magnetophoretic mobility of the CSC and NSTC samples after 24 hours and 48 hours of culturing in 6.20 mM Fe.

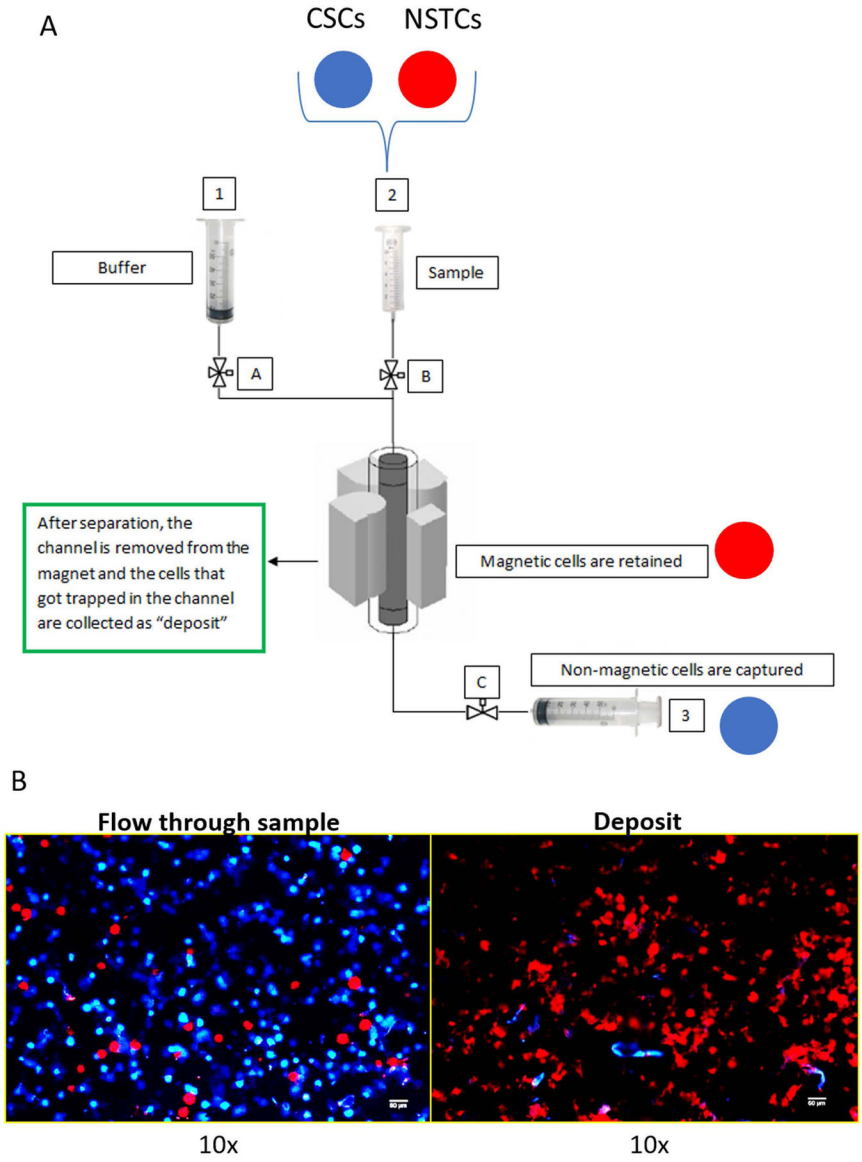

Fig. 4.

4A: Diagram of the quadrupole, magnetic cell separation system, QMS. Consistent with the fluorescent cell tracker dyes used in the separation studies, blue and red circles representing the locations of the CSCs and NSTCs are included. 4B: Microscopic images of the stained cells collected in flow through exit stream, and the cells deposited on the wall and subsequently washed out.

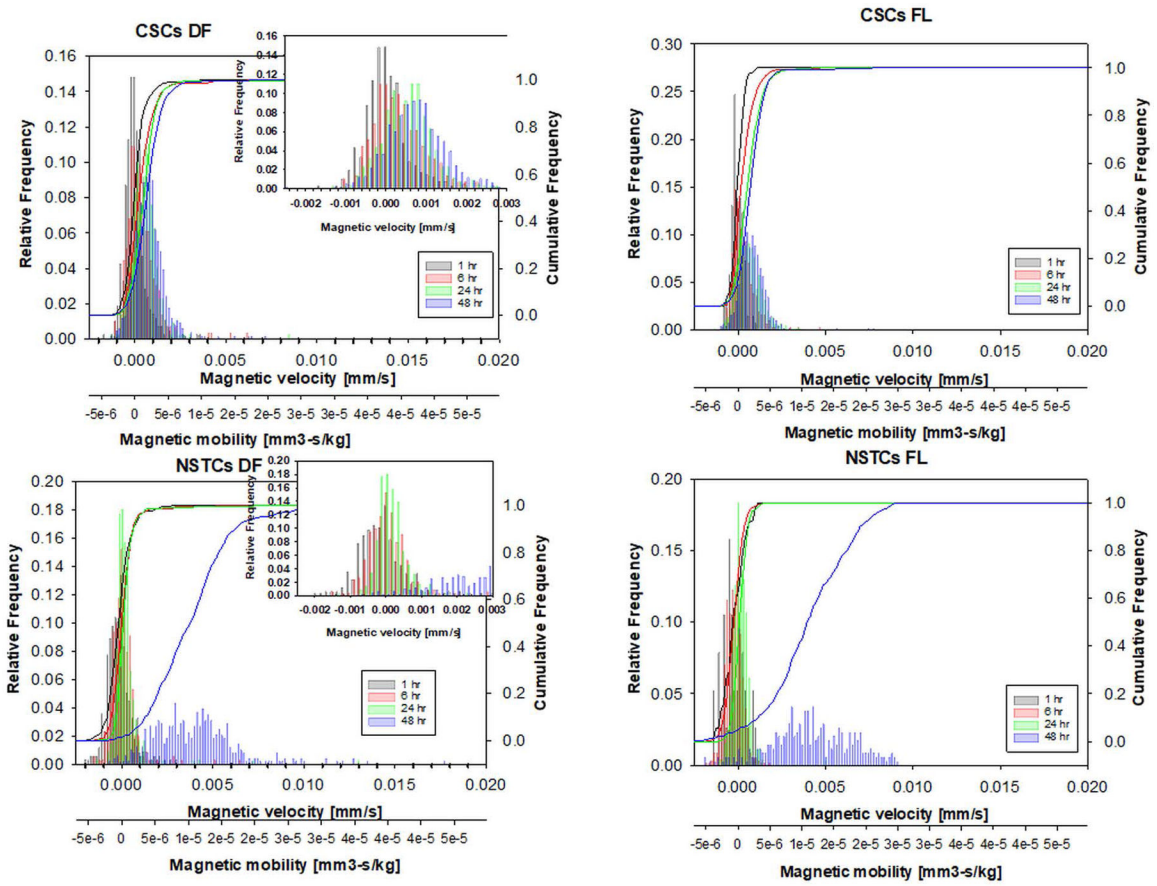

Fig. 5.

Histograms of the magnetic velocity and magnetophoretic mobility of the CSC and NSTC samples after 1, 6, 24, and 48 hours of culturing in 2.1 mM Fe.

Table 1.

Iron- and glucose-supplemented culture media

	Fe(NO3)3 Concentration		Glucose Concentration	
Condition #	**[mg/ml]**	**[mM]**	**[mg/ml]**	**[mM]**
1	0–0.00001 *	0–0.0004 *	4.5 *	25 *
2	0.5	2.07	4.5 *	25 *
3	1.50	6.20	4.5 *	25 *
4	0–0.00001 *	0–0.0004 *	45.0	250

* amount in normal media

Table 2.

Summary of four separation experiments

Trial #	Cells loaded in 2 ml	Input ratio(CSCs:NSTCs)	Flowrate for collection	Enrichment ratio(CSCs:NSTCs)
1	$2 * 10^4$ cells	1:1	10 ml/min	16:1
2	$1.5 * 10^5$ cells	2:1	20 ml/min	4.1:1
3	$1.5 * 10^5$ cells	2:1	10 ml/min	5.1:1
4	$1.5 * 10^5$ cells	2:1	10 ml/min	16:1